Ab-initio prediction of magnetoelectricity in infinite-layer iron oxides

Kunihiko Yamauchi[1], Tamio Oguchi[1,2], and Silvia Picozzi[3]
1. ISIR-SANKEN, Osaka University, 8-1 Mihogaoka, Ibaraki, Osaka, 567-0047, Japan
2. CREST, JST, 5 Sanbancho, Chiyoda-ku, Tokyo, 102-0075, Japan
3. Consiglio Nazionale delle Ricerche (CNR-SPIN), 67100 L'Aquila, Italy
(Dated: April 5, 2013)

Density functional based simulations are employed to explore magnetoelectric effects in iron-based oxides, showing a unique layered structure. We theoretically predict $CaFeO_2$ to be a promising magnetoelectric, showing magnetically-controlled large electric polarization, possibly even above room temperature. The cross coupling between magnetic and dipolar degrees of freedom needs, as main ingredients, Fe-site spin-orbit coupling and a spin-dependent O p - Fe d hybridization, along with structural constraints related to the non-centrosymmetric point group and the peculiar geometry characterized by "flattened" FeO_4 tetrahedrons. In order to enhance magnetoelectric effects, we performed a materials-design leading to a novel and optimized system, $MgFeO_2$, where the larger O_4 tetrahedral distortion leads to a stronger polarization.

PACS numbers: Valid PACS appear here

Introduction. — Aiming at the mutual control of electricity and magnetism, the magnetoelectric (ME) coupling between the magnetic order parameter (M) and the ferroelectric one (P) has been well studied in recent years in the context of *multiferroic* oxides. [1] Microscopically, common mechanisms for ME effects can be classified into either the inverse Dzyaloshinskii-Moriya mechanism [2] (or the equivalent spin-current mechanism [3]) showing $\boldsymbol{P} \propto \sum_{ij} \boldsymbol{e}_{ij} \times (\boldsymbol{S}_i \times \boldsymbol{S}_j)$ between neighboring spins connected by a vector $\boldsymbol{e}_{ij}$, or the inverse Goodenough-Kanamori (or exchange-striction) mechanism [4] showing $\boldsymbol{P} \propto \sum_{ij} J_{ij}(\boldsymbol{S}_i \cdot \boldsymbol{S}_j)$ with exchange integral J_{ij}. Recently, an alternative mechanism, denoted as "spin-dependent p-d hybridization" was proposed.[5, 6] There, the spin-orbit-coupling (SOC) "asymmetrizes" the p-d hybridization between the transition metal (TM) and the surrounding ligands, inducing an electric polarization $\boldsymbol{P} \propto \sum_{ij} (\boldsymbol{S}_i \cdot \boldsymbol{e}'_j)^2 \boldsymbol{e}'_j$, where $\boldsymbol{e}'_j$ labels the vectors connecting the TM to the ligand ions, which explains ferroelectricity in $CuFeO_2$. It has been more recently reported that the mechanism can be responsible for the polarization observed in $Ba_2CoGe_2O_7$ (BCGO), where two neighboring Co spins are aligned in an antiferromagnetic (AFM) configuration,[7] as confirmed by our previous DFT study.[8] In fact, in the CoO_4 tetrahedral coordination, the occupied *non-bonding* $x^2 - y^2$ state for minority spins is mixed with unoccupied *bonding* yz and zx states through SOC, leading to *asymmetric pd hybridization* and, in turn, to a net polarization. Incidentally, we found a relevant ME mechanism in magnetite, Fe_3O_4, where the complicated charge-ordering pattern with polar Cc space group causes a large spontaneous polarization, whereas SOC causes a small spin-dependent change in the polarization under the ferrimagnetic order.[9]

Guided by the same theoretical analysis performed for BCGO and Fe_3O_4, in the search for novel ME materials, we identified the requirements for the spin-dependent pd hybridization mechanism as follows: i) a non-polar but non-centrosymmetric point symmetry at magnetic sites, whose symmetry is lowered into polar group under a specified magnetic order; ii) weak magnetic anisotropy (so that spins easily follow the magnetic field), at least in a plane, iii) strong pd hybridization and strong SOC needed to achieve a large ME effect. Whereas the third condition can be fulfilled by using either $4d$ or $5d$ elements instead of $3d$ transition metals, our approach consists in exploring different crystal structures to enhance the asymmetric pd hybridization to realize larger polarization.

Our strategy is rather simple. We searched for oxides which have space group similar to BCGO and identified $CaFeO_2$ as a promising candidate. Indeed, $CaFeO_2$ crystalizes in *non-centrosymmetric and non-polar* $P\overline{4}2_1m$ (#113) tetragonal layered structure. The crystal structure shows peculiar FeO_4 squares heavily distorted to tetrahedrons (Fig. 1 (a)). Experimentally it can be synthesized by removing only apical oxygens from FeO_6 structure in precursor Brownmillerite $CaFeO_{2.5}$ by using reductive hydride CaH_2. The peculiar FeO_4 tetrahedron is unique to $CaFeO_2$. For example, no distortion has been reported in the infinite-layer cuprate $ACuO_2$ (A= Ca, Sr, Ba), well studied in the context of high-temperature superconductivity[10], as well as $SrFeO_2$, having high-spin Fe ions in planar square coordination.[11] So far, the recently synthesized $CaFeO_2$ uniquely shows the corrugation of FeO_2 planes, where the O ion is slightly deviated by 0.32Å from the ab plane.[12]

We note that $CaFeO_2$ exhibits G-type antiferromagnetic order (both in-plane and inter-plane AFM coupling) below a remarkably high Néel temperature, T_N=420K — even above room temperature—. Four Fe atoms in the unit cell, Fe1 at (0, 0, 0), Fe2 at (1/2, 1/2, 0), Fe3 at (0, 0, 1/2), and Fe4 at (1/2, 1/2, 1/2), are responsible

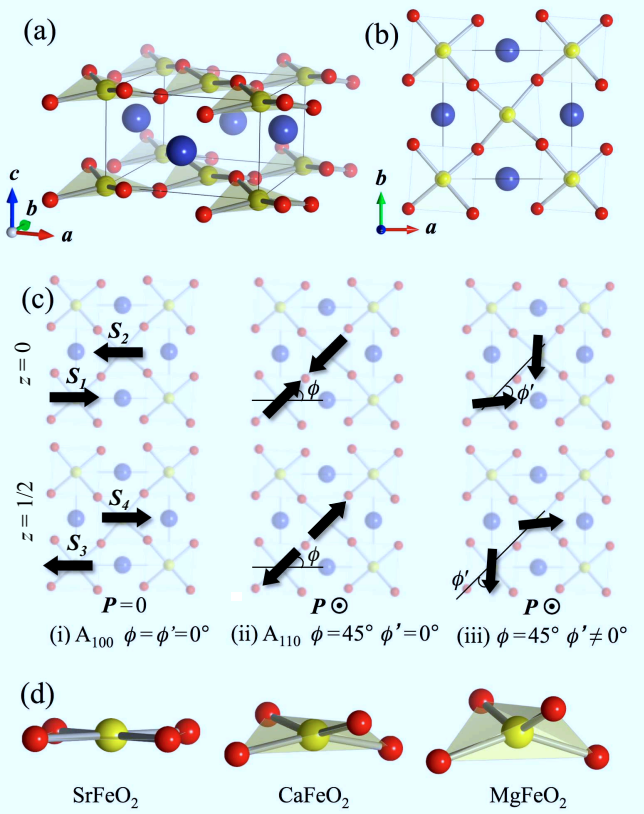

FIG. 1: (a) Crystal structure and (b) projected image in the ab plane of $CaFeO_2$ with the P-42_1m space group; Fe ions (located in flat O_4 tetrahedrons) lie in c=0 planes whereas Ca ion lies in c=1/2 planes. (c) Fe spin configurations: (i), (ii) collinear AFM and (iii) non-collinear spin-canted under applied $\boldsymbol{H}$//1-10. Note that the AFM inter-layer coupling is not shown here. (d) Development of MO_4 tetrahedron with respect to the planar square coordination by substituting M by Sr, Ca and Mg.

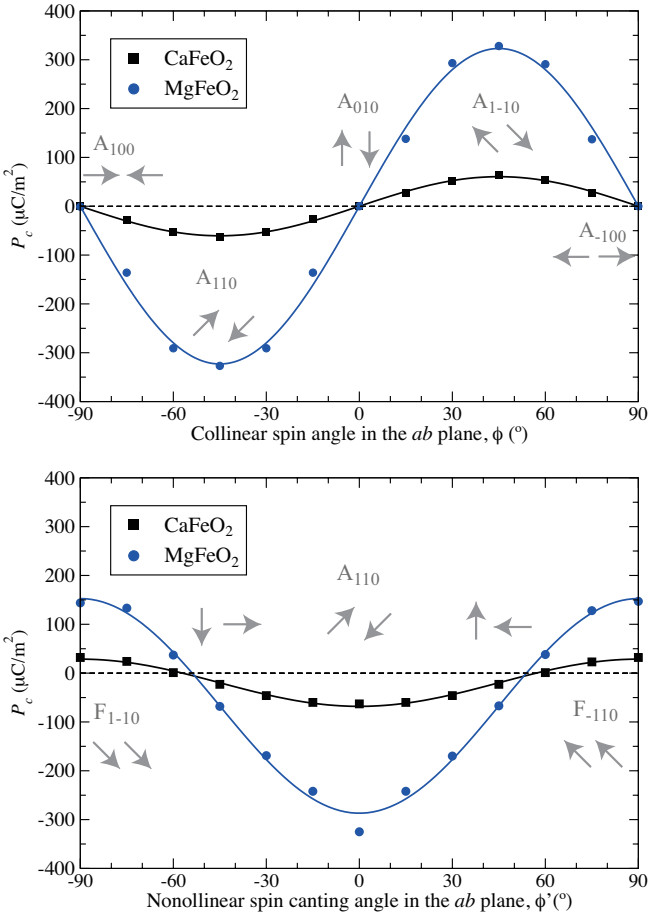

FIG. 2: (a) DFT results for $\boldsymbol{P}_c$ as a function of the *collinear* spin angle ϕ in the ab plane, fitted to sine curves. Spin configurations in the ab plane shown by arrows. (b) DFT results for $\boldsymbol{P}_c$ as a function of the *noncollinear* spin-canting angle ϕ' in the ab plane, fitted to cosine curves (solid line).

for the magnetism (the magnetic unit cell is double along the c axis compared to the structural unit cell).

In this study, by means of DFT calculations, we first investigate the steric effect of A site substitution (A= Mg, Ca, Sr, Ba) in $AFeO_2$ and the stability of the infinite-layer structure; then, we investigate the ME effect induced by varying the magnetic order under SOC.

Symmetry Analysis. — Although the space group of crystal structure of $CaFeO_2$ is the same as BCGO, the G-type AFM order may give a different ME behavior compared to the C-type (only in-plane AFM coupling) AFM order in BCGO. In order to characterize possible ME effects, we first briefly perform a group theory analysis and discuss its implications in the framework of Landau theory of phase transitions.[13] In the parent $P\overline{4}2_1m1'$ space group with eight symmetry operations $\{E,\ C_{2(z)},\ 2S_4,\ 2C_{2(x,y)},\ 2\sigma_d\}$ plus time-reversal $\{1'\}$, the magnetic order leads to a lowered symmetry. We define the order parameters $\boldsymbol{F} = \boldsymbol{S}_1 + \boldsymbol{S}_2 + \boldsymbol{S}_3 + \boldsymbol{S}_4$ and $\boldsymbol{A} = \boldsymbol{S}_1 - \boldsymbol{S}_2 - \boldsymbol{S}_3 + \boldsymbol{S}_4$ as the ferromagnetic (FM) and G-type AFM combination of Fe1..4 spins, respectively. Since the G-type AFM order doubles the unit cell along the c direction, we have to take into account the c translation $\{c = +(001)\}$ in this analysis. (*i.e.* AFM order is not invariant under the c translation.)

Using the transformation rules given in Table I, the thermodynamic free energies in terms of all the possible ME coupling terms (of the form $\boldsymbol{P}\cdot\boldsymbol{M}^2$, which are invariant under any symmetry operations) results in the simple exression:

$$F_{\rm ME} = c_{\rm A} P_c A_a A_b + c_{\rm F} P_c F_a F_b. \qquad (1)$$

The dielectric energy is written as $F_{\rm DE} = -\boldsymbol{P}^2/2\chi$. Here, c_A, c_F and χ (henceforth set as 1) are constants. $\boldsymbol{P}$ is then evaluated at the minima of $F = F_{\rm ME} + F_{\rm DE}$, reading

$$P_a = P_b = 0, \qquad P_c = c_{\rm A} A_a A_b + c_{\rm F} F_a F_b. \qquad (2)$$

We observe that this result means that P_c can originate from either FM or AFM order, but not from their

TABLE I: Matrices of the generators of space group $P\bar{4}2_1m1'$ in the representations spanned by F, A, and P. The group elements denote the identity, π-rotation, $\pi/2$-rotoinversion $S_4^-(=IC_{4z}^-)$, screw $C_{2y}+(\frac{1}{2}\frac{1}{2}0)$, time-reversal $1'$ and translation c. Labels of irreducible representation (IR) are taken from the ISODISTORT program.[14]

	E	C_{2z}	S_4^-	C_{2y}	$1'$	c	IR
F_a	1	−1	$\begin{bmatrix}0 & 1\\ -1 & 0\end{bmatrix}$	−1	−1	1	$m\Gamma_5 E_1^* a$
F_b	1	−1		1	−1	1	$m\Gamma_5 E_1^* b$
F_c	1	1	1	−1	−1	1	$m\Gamma_4 A$
A_a	1	−1	$\begin{bmatrix}0 & -1\\ 1 & 0\end{bmatrix}$	−1	−1	−1	$mZ_5 E_{(1,2)}^*$
A_b	1	−1		1	−1	−1	$mZ_5 E_{(1,2)}^*$
A_c	1	1	−1	−1	1	−1	$mZ_1 Aa$
P_a	1	−1	$\begin{bmatrix}0 & -1\\ 1 & 0\end{bmatrix}$	−1	1	1	Γ_5
P_b	1	−1		1	1	1	Γ_5
P_c	1	1	−1	−1	1	1	Γ_3

combination.

From now on, we will focus on the P_c behavior assuming a canted AFM configuration under an applied magnetic field, i.e., we first simultaneously counter-clock-wise rotate four Fe spins in the ab plane keeping the AFM order with the angle ϕ from the a axis, then we cant spins by an angle ϕ', as depicted in Fig. 1. Accordingly, we set $\boldsymbol{S}_1 = \boldsymbol{S}_4 = S(\cos(\phi+\phi'), \sin(\phi+\phi'), 0)$ and $\boldsymbol{S}_2 = \boldsymbol{S}_3 = S(-\cos(\phi-\phi'), -\sin(\phi-\phi'), 0)$, ending up with

$$P_c = 4aS^2 \sin 2\phi \,(\cos 2\phi' + b)\,, \tag{3}$$

where $a = c_{\rm A} + c_{\rm F}$ and $b = c_{\rm A} + c_{\rm F} - 2$.

A spontaneous P_c is therefore induced in the A_{110} or A_{1-10} (ϕ=±45°) order but not in the A_{100} (A_{010}) one. Analogously to previous studies [8, 9], the nonmagnetic group lacks inversion symmetry, but the symmetries which prohibit P_c (e.g. C_{2y} rotation) are broken by the A_{110} magnetic order. Finally, Eq. (3) at fixed ϕ (ϕ') gives the simple $\phi'(\phi)$-dependence, $P_c(\phi) \propto \sin 2\phi$ and $P_c(\phi') \propto \cos 2\phi'$. This result shows a slightly different aspect from the P induced in C-AFM BCGO[7, 8], where $P_c^{\rm BCGO}(\phi') \propto \cos(2\phi'-\beta)$ and the phase shift β depends on the non-zero $c_{\rm AF}$ coefficient. Notably, the phase shift of the cosine curve, β, is lost in G-AFM $CaFeO_2$. Physically, a close inspection of the magnetic and ionic configuration shows that the cancellation is due to the C type interlayer AFM coupling and the consequent spin canting pattern in different layers (see Fig. 1(c)-(iii)).

DFT analysis — In order to quantitatively confirm the ME behavior, we performed DFT calculations on AFeO$_2$ (A = Mg, Ca, Sr, Ba) by using the VASP code[15] with GGA-PBE+U potential (U=4 eV for Fe-d state, taken from Ref.[12]). Note that bare GGA calculations result in quasi-metallic state with small gap, *e.g.* $E_g \lesssim$0.1eV in $MgFeO_2$. After structural optimization under G-AFM configuration without SOC, we found that $MgFeO_2$ and $CaFeO_2$ show a corrugation in the FeO_2 layer in non-centrosymmetric P-42$_1m$ structure, whereas

TABLE II: Magnetic anisotropy energy (MAE) (meV/Fe) obtained by comparing the total energy with different spin directions under SOC and for different values of U in the GGA+U scheme. Spin and orbital moment (S and L) ($\mu_{\rm B}$) are also reported for S//(100).

	E(100)	E(110)	E(001)	S	L
$CaFeO_2$	0	0.00	+2.03	3.61	0.09
$MgFeO_2$	0	+0.60	+2.90	3.61	0.10

$SrFeO_2$ and $BaFeO_2$ show a "flat" layer in centrosymmetric $P4/mmm$ structure. In the FeO_4 tetrahedra of $MgFeO_2$ and $CaFeO_2$, the JT-active Fe^{2+} (d^6) ion shows $e_g^{2\uparrow} t_{2g}^{3\uparrow} e_g^{1\downarrow} t_{2g}^{0\downarrow}$ occupied orbital states, where the almost-non-bonding $3z^2-r^2$ states perpendicular to the ab plane is the lowest energy orbital state. (Here we choose a local frame $\mathbf{x}$//$\mathbf{a}$, $\mathbf{y}$//$\mathbf{b}$, $\mathbf{z}$//$\mathbf{c}$ and neglect the small tilting of O_4 tetrahedra with respect to the crystalline axis.) The calculated small magnetic anisotropy in the easy ab plane and hard c axis (Tbl. II) grant an easy control over the spins by applied magnetic field, $\boldsymbol{H}$; even under a small magnetic field, the spins flop to be perpendicular to $\boldsymbol{H}$ and then cant in order to reduce the Zeeman energy.

Imposing the collinear AFM configuration, we simultaneously rotate the Fe spins in the ab plane. We evaluated the ME effect as the change of $\boldsymbol{P}$ (calculated by Berry phase method[16]) induced by the rotation of $\boldsymbol{M}$ with respect to the crystalline axes, including the optimization of the atomic coordinates. Figure 2 (a) shows P_c as a function of the spin-rotation angle ϕ: it is consistent with the previously discussed Landau analysis, being $P_c \propto \sin 2\phi$. As summarized in Tbl.III, the purely electronic contribution via SOC at fixed atomic structure, $P_{\rm elec}$=13μC/m^2, is strongly enhanced (up to 62μC/m^2) when internal atomic coordinates are optimized. This situation is similar to previously reported calculations on multiferroic $TbMnO_3$, where the purely electronic contribution $P^{\rm elec}$=32$\mu C/m^2$ is enhanced up to $P^{\rm elec+ion}$=-467$\mu C/m^2$ by ionic relaxation.[17] In $CaFeO_2$, the maximum value of the calculated polarization is 62μC/m^2, slightly larger than the corresponding value in BCGO (P=47μC/m^2). Furthermore, $MgFeO_2$ is predicted to show a much larger polarization, P=327μC/m^2, comparable with $TbMnO_3$.

TABLE III: Deviation of Fe-O-Fe bond angle from square configuration and P_c under A_{110} magnetic ordering, calculated in the fixed non-polar atomic structure ($P_{\rm exp}$) and with optimized polar structure ($P_{\rm opt}$). Experimentally, the P_c in A_{110} $Ba_2CoGe_2O_7$ is about 100μC/m^2[7], whereas polarization in $CaFeO_2$ and $MgFeO_2$ has not been measured.

	BCGO	$SrFeO_2$	$CaFeO_2$	$MgFeO_2$
180-∠FeOFe (°)	—	0	20.8	34.7
$P_{\rm fix}$ (μC/m^2)	10	0	13	22
$P_{\rm opt}$ (μC/m^2)	47	0	62	327

The strong increase of P in $MgFeO_2$ is attributed to the larger O_4 tetrahedral distortion with respect to the centrosymmetric flat layer structure. In fact, we also performed calculations on $BeFeO_2$, showing even more distorted tetrahedrons. Whereas we estimated a significantly large polarization, $P{\sim}2000\mu C/m^2$, the chemical stability of the crystal structure with such a small ionic radius ion is questionable. It is shown in Tbl.III that the ionic contribution (mostly oxygen ionic displacement) plays a crucial role in total P. The structural difference of iron-based oxides compared to BCGO is that FeO_4 tetrahedra are corner-shared, whereas CoO_4 tetrahedra are intercalated by GeO_4 tetrahedra in BCGO. This leads to a cooperative effect between neighboring FeO_4 tetrahedra, so as to enhance the ionic displacement of O ion shared by two FeO_4 tetrahedra.

The ionic displacement driven under A_{110} magnetic order in $CaFeO_2$ is characterized by two phonon modes, Γ_1 and Γ_3. While the Γ_1 phonon mode doesn't change the original space group, the Γ_3 mode reduces the sparse group from $P\text{-}42_1m1'$ to polar $Cmm21'$. Under the Γ_3 phonon mode, $MgFeO_2$ exhibits Mg and O ionic displacements: both ions are shifted along the z direction, by 0.0006 Å and by 0.0011 Å, respectively (displacements characterized by $A1(1)$ and $A_2'(a)$). This means that ferroelectricity is strongly coupled, through magnetism, with lattice distortions in a sort of *magnetostrictive-piezoelectric effect*.

We look then at the spin-canting effect induced by an applied field H_{110}. Figure 2 (b) shows the change in P_c induced by artificially canting the spins by an angle ϕ', starting from the A_{1-10} AFM configuration. In agreement with the Landau theory analysis, P_c evolves as $\cos 2(\phi') + \text{const.}$,

Single-site SOC induced ME effect — The microscopic origin of $\boldsymbol{P}$ in $CaFeO_2$ can be explained in terms of spin-orbit coupling term treated as second order perturbation. In the flat tetrahedral FeO_4 coordination (Fe is at $2a$ site with $-4..$ symmetry), Fe-d electrons occupy $3z^2-r^2$, x^2-y^2, degenerate yz/zx, and xy orbital states in order, which is consistent with order of the nonbonding (*i.e.* spatially avoiding O ligands) character.[19] Comparing the DOS of $CaFeO_2$ and $MgFeO_2$, the electronic structures are very similar, although the crystal field splitting between $3z^2-r^2$ and x^2-y^2 $(=\Delta_1)$ is comparatively weakened in more tetragonally distorted $MgFeO_2$.

The spin orbit coupling (SOC) term is described as $H_{\rm SOC} = \lambda \sum_{\alpha,\alpha'} \langle\alpha| L\cdot S |\alpha'\rangle\, d^\dagger_\alpha d_{\alpha'}$, where the matrix elements can be expressed as a function of the polar and azimuthal angles (θ,ϕ) defining a local reference for the spin-quantization axis[18]. SOC-induced mixing of the local d levels between occupied and unoccupied states lifts the degeneracies of yz and zx manifolds and implies asymmetric hybridizations with the ligand oxygens, that ultimately induces a local dipole moment along the c axis. Large SOC mixing is expected at Δ_1 between $|3z^2-r^2\downarrow\rangle$ and $|x^2-y^2\downarrow\rangle$, Δ_2 between $|xy\uparrow\rangle$ and $|x^2-y^2\downarrow\rangle$ and Δ_3 between $|xy\uparrow\rangle$ and $|yz,zx\downarrow\rangle$, shown in Fig.3. Among them, Δ_1 and Δ_3 are relevant to ferroelectricity. Under this SOC-related mixing, the occupied states are modified by small contribution from the unoccupied states;

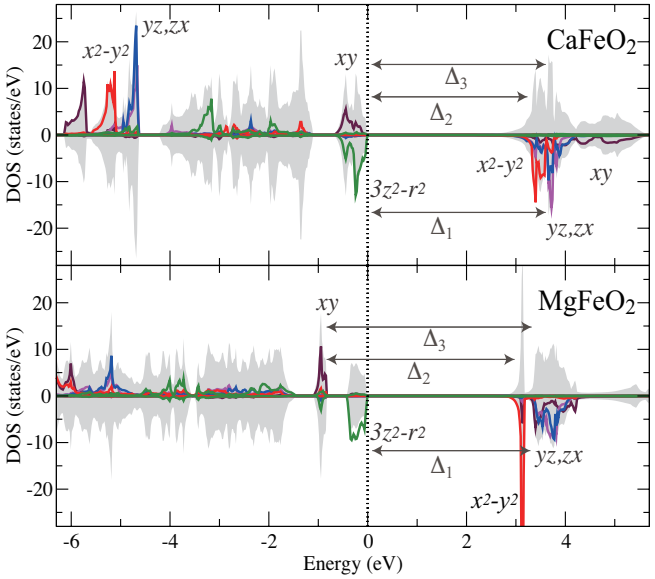

FIG. 3: Density of states (DOS) around the Fermi energy (E=0) of $CaFeO_2$ and $MgFeO_2$. The d-orbital projected DOS and SOC mixing between occupied and unoccupied states are labeled.

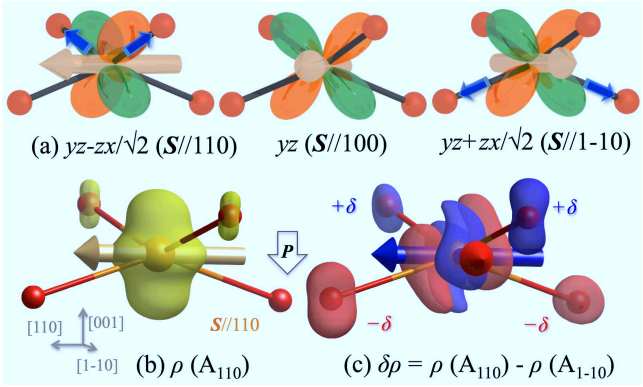

FIG. 4: (a) Schematic picture of unoccupied Fe-d orbital state which is mixed into occupied state under SOC. The orbital shape changes by rotating Fe spin. (b) Charge density isosurface of the highest occupied band (i.e. Fe-d $3z^2$-r^2 orbital state) in $MgFeO_2$ under A_{110} magnetic order. Spin direction is shown by an orange arrow. (c) Change in the charge density ($\delta\rho$) by rotating Fe spin from [110] to [1-10] direction (positive shown in blue color; negative, in red). Direction of polarization caused by the charge difference ($\pm\delta$) is shown by an open arrow. SOC is enhanced by factor of 10.

$$\delta \left|3z^2 - r^2\downarrow\right\rangle = -\frac{\sqrt{3}i\lambda}{2\Delta_1}\left(\cos\phi\left|yz\downarrow\right\rangle - \sin\phi\left|zx\downarrow\right\rangle\right) \quad (4)$$

$$\delta \left|xy\uparrow\right\rangle = -\frac{\lambda}{2\Delta_3}\left(\cos\phi\left|yz\downarrow\right\rangle + \sin\phi\left|zx\downarrow\right\rangle\right), \quad (5)$$

where θ is already set as 90°. Comparing the coefficients in above equations 4-5 and considering Δ_1 and Δ_3 to have a similar magnitude (see Fig.3), we observe that the SOC mixing involving Δ_1 contributes to the change in orbital occupancy from the change in spin azimuth angle ϕ by an amount which is about 3 times larger than the SOC mixing involving Δ_3. Therefore, the energetically highest occupied state $\left|3z^2 - r^2\downarrow\right\rangle$ is mixed with unoccupied $(\cos\phi\left|yz\downarrow\right\rangle + \sin\phi\left|zx\downarrow\right\rangle)$ orbital states, which modifies the shape according to the spin rotation (see Fig.4 (a)). This gives rise to the asymmetric *pd* hybridization, enhancing the bonding character with upper oxygen states (when **S**//[110]) or with lower oxygen states (when **S**//[1-10]). The change in the charge density of the occupied state by spin rotation indeed exhibits an asymmetric *pd* hybridization (shown in Fig. 4 (c)). In this way, a local dipole, $p_c \propto \sin 2\phi$, develops along c, as predicted from the functional form, $\boldsymbol{P} \propto \sum_{ij}(\boldsymbol{S}_i \cdot \boldsymbol{e}'_j)^2\, \boldsymbol{e}'_j$. [5–7] Such a mixing of local *d*-levels nicely explains why the P_c size is maximum at $\phi = \pm 45°$, when the Co spin is parallel either to the upper- or to the lower-lying oxygen bond; indeed, as pictorially shown in Fig. 4 (a), the composition of yz and zx orbitals has an asymmetric bonding nature in the tetrahedron, i. e. non-bonding with upper ligands and bonding with lower ligands or vice versa.

Conclusions — On the grounds of the known microscopic mechanism underlying peculiar magnetoelectricity observed in $Ba_2CoGe_2O_7$, we predict much stronger magnetoelectric effects to appear in iron-based oxides, such as $CaFeO_2$, where a large polarization - magnetically controllable - is estimated. In addition to essential ingredients, such as spin-dependent $p-d$ hybridization and spin-orbit coupling, here a central role is played by the peculiar geometry, featuring "flattened" FeO_4 tetrahedrons and non-centrosymmetric point group. The latter conditions are optimized in $MgFeO_2$, where our materials-design approach leads to magnified magnetoelectric effects, with a giant polarization tuned by magnetic fields.

The research leading to these results has received funding from a Grant-in-Aid for Young Scientists (B) from Japan Society for the Promotion of Science (JSPS) under Contract No. 24740235 and from JST, CREST "Creation of Innovative Functions of Intelligent Materials on the Basis of the Element Strategy". The computation in this work has been done using the facilities of the Supercomputer Center, Institute for Solid State Physics, University of Tokyo.

[1] M. Fiebig, J. Phys. D: Appl. Phys. **38** R123 (2005).
[2] I. A. Sergienko and E. Dagotto, Phys. Rev. B **73**, 094434 (2006).
[3] H. Katsura, N. Nagaosa, and A. V. Balatsky, Phys. Rev. Lett. **95**, 057205 (2005).
[4] T. Arima et al., Phys. Rev. Lett. **96**, 097202 (2006).
[5] T. Arima, J. Phys. Soc. Jpn. **76**, 073702 (2007).
[6] C. Jia, et. al., Phys. Rev. B **76**, 144424 (2007).
[7] H. Murakawa et al. Phys. Rev. Lett. **105**, 137202 (2010).
[8] K. Yamauchi, P. Barone, and S. Picozzi, Phys. Rev. B **84**, 165137 (2011).
[9] K. Yamauchi and S. Picozzi, Phys. Rev. B **85**, 085131 (2012).
[10] M. Azuma, *et al.*, Nature **356**, 6372 (1992).
[11] Y. Tsujimoto, *et. al.*, Nature **450**, 1062 (2007).
[12] C. Tassel, *et. al.*, J. Am. Chem. Soc. **131**, 221, (2009).
[13] L. D. Landau and E. M. Lifshitz, Statistical Physics, Part I (Pergamon Press, Oxford, 1980).
[14] B. J. Campbell et al, J. Appl. Cryst. **39**, 607 (2006).
[15] G. Kresse and J. Furthmüller, Phys. Rev. B **54**, 11169 (1996).
[16] R.D.King-Smith and D.Vanderbilt, Phys. Rev. B **47**, 1651 (1993); R. Resta, Rev. Mod. Phys **66**, 899 (1994).
[17] A. Malashevich and D. Vanderbilt, Phys. Rev. Lett. **101**, 037210 (2008).
[18] H. Takayama, K bohnen and P. Fulde, Phys. Rev. B **14**, 2287 (1976).
[19] In this study, we set x, y, z axis parallel to a, b, c axis, respectively, as neglecting the small tilting of the O_4 tetrahedron in the ab plane.